

Electric-octupole and pure-electric-quadrupole effects in soft-x-ray photoemission

A. Derevianko,^{1,*} O. Hemmers,² S. Oblad,² P. Glans,³ H. Wang,⁴ S. B. Whitfield,⁵ R. Wehlitz,⁶ I. A. Sellin,⁷ W. R. Johnson,¹ and D. W. Lindle²

¹*Department of Physics, University of Notre Dame, Notre Dame, IN 46556*

²*Department of Chemistry, University of Nevada, Las Vegas, NV 89154-4003*

³*Atomic Physics, Stockholm University, 10405 Stockholm, Sweden*

⁴*Department of Physics, Uppsala University, Box 530, S-751 21 Uppsala, Sweden*

⁵*Department of Physics, University of Wisconsin, Eau Claire, WI 54702*

⁶*Synchrotron Radiation Center, University of Wisconsin, Stoughton, WI 53589*

⁷*Department of Physics, University of Tennessee, Knoxville, TN 37996*

(December 16, 2017)

Second-order [$O(k^2)$, $k = \omega/c$] nondipole effects in soft-x-ray photoemission are demonstrated via an experimental and theoretical study of angular distributions of neon valence photoelectrons in the 100–1200 eV photon-energy range. A newly derived theoretical expression for nondipolar angular distributions characterizes the second-order effects using four new parameters with primary contributions from pure-quadrupole and octupole-dipole interference terms. Independent-particle calculations of these parameters account for a significant portion of the existing discrepancy between experiment and theory for Ne $2p$ first-order nondipole parameters.

PACS: 32.80.Fb, 31.25.Eb

A mainstay of photoemission is the (electric-)dipole approximation (DA), in which all higher-order multipoles are neglected [1]. The range of validity of the DA has received renewed interest as recent experiments [2,3] uncovered breakdowns at progressively lower photon energies. At high energies ($\hbar\omega > 5$ keV), breakdown of the DA in photoionization is well-known, and a proper description requires inclusion of many multipoles [4]. For soft-x-ray ($\hbar\omega < 5$ keV) photoionization, in contrast, first-order [$O(k)$] corrections to the DA generally have been considered sufficient [5]. At these relatively low energies, DA breakdown primarily leads to forward/backward asymmetries in photoelectron angular-distribution patterns. Especially striking have been observations of nondipole effects at energies below 1 keV [3], a region in which the DA is usually considered valid. In the present work, an experimental and theoretical analysis of neon valence photoemission demonstrates a new, and unexpected, breakdown: significant second-order [$O(k^2)$] nondipole effects, primarily due to electric-octupole and pure-electric-quadrupole interactions, in low-energy photoemission.

We begin with Cooper's $O(k)$ formula for the differential photoionization cross section of a subshell (n, κ) in a randomly oriented target using linearly polarized light [6]:

$$\frac{d\sigma_{n\kappa}}{d\Omega} = \frac{\sigma_{n\kappa}}{4\pi} \left\{ 1 + \beta_{n\kappa} P_2(\cos\theta) + (\delta_{n\kappa} + \gamma_{n\kappa} \cos^2\theta) \sin\theta \cos\phi \right\}, \quad (1)$$

where $\sigma_{n\kappa}$ is the photoionization cross section, $\beta_{n\kappa}$ describes the angular distribution within the DA, and $\delta_{n\kappa}$ and $\gamma_{n\kappa}$ are nondipole angular-distribution parameters characterizing the leading first-order corrections to the DA (mostly $E_2 - E_1$ terms). The angles θ and ϕ are determined by the direction of the photoelectron relative to the photon-polarization $\hat{\epsilon}$ and photon-propagation \mathbf{k} directions, respectively. The first two terms on the right of Eq. (1) constitute the usual DA expression for the differential cross section, and the DA notion of a "magic angle" [$\theta_m = 54.7^\circ$, $P_2(\cos\theta_m) = 0$] is preserved only in the $\phi = 90^\circ$ plane perpendicular to \mathbf{k} .

At this level of approximation, recent rare-gas experiments [2,3] observed significant modifications of photoelectron angular distributions from DA expectations, generally in good agreement with first-order independent-particle-approximation (IPA) calculations [6,7]. The only exception is Ne $2p$ [3]; while measured values of γ_{2s} (δ_{2s} is negligible when $\beta_{2s} = 2$) agree fairly well with calculations, measured values of the combined parameter ζ_{2p} ($= 3\delta_{2p} + \gamma_{2p}$) are 30% larger than IPA predictions for energies near 1 keV.

The same experiment also found β_{2p} disagrees substantially with IPA calculations in this energy region, but is in close agreement with correlated calculations using the

random-phase approximation (RPA) [8,9], thereby identifying important electron-correlation effects well above the $n = 2$ thresholds [10]. This result led to speculation [3] the discrepancy between measured and IPA-calculated ζ_{2p} values might also be due to interchannel-coupling effects. However, subsequent first-order nondipole calculations including electron correlation [11] disproved this notion; RPA values of Ne ζ_{2p} are in excellent agreement with the uncorrelated IPA results [6,7].

In this work, we explain much of this discrepancy between theory and experiment for Ne ζ_{2p} . Beginning with theory, second-order [$O(k^2)$] corrections to the differential cross section, which arise from interferences between $E_1 - E_3$, $E_1 - M_2$, $E_2 - E_2$, $E_2 - M_1$, and $M_1 - M_1$, and from retardation corrections to $E_1 - E_1$ amplitudes, are incorporated into Eq. (1):

$$\frac{d\sigma_{n\kappa}}{d\Omega} = \frac{\sigma_{n\kappa}}{4\pi} \left\{ 1 + (\beta_{n\kappa} + \Delta\beta_{n\kappa}) P_2(\cos\theta) + (\delta_{n\kappa} + \gamma_{n\kappa} \cos^2\theta) \sin\theta \cos\phi + \eta_{n\kappa} P_2(\cos\theta) \cos 2\phi + \mu_{n\kappa} \cos 2\phi + \xi_{n\kappa} (1 + \cos 2\phi) P_4(\cos\theta) \right\}, \quad (2)$$

where the $O(k^2)$ -parameters $\Delta\beta, \eta, \mu$, and ξ are introduced [12]. Three of them satisfy the constraint $\eta + \mu + \xi = 0$. Reference [12] contains complete formulae and a tabulation of first- and second-order parameters for all subshells of the rare gases helium to xenon.

For experiment, we first present results for Ne γ_{2s} and ζ_{2p} determined assuming only first-order corrections, embodied in δ and γ , are needed to correctly interpret the data. The experiments were performed with an apparatus designed to measure deviations from the DA [13]; γ_{2s} and ζ_{2p} are determined using angle-resolved photoemission intensities at θ_m and both $\phi = 0^\circ$ and $\phi = 90^\circ$. Figure 1 compiles old [3] and new values for ζ_{2p} and γ_{2s} (open squares) determined in this way. The solid curves represent $O(k)$ calculations [6,7,11], which agree well with the $2s$ results, but disagree with the $2p$ results above 800 eV.

To obtain $O(k^2)$ predictions (dotted curves in Fig. 1), we first carried out numerical IPA studies of second-order corrections for neon. Wavefunctions for bound-state and continuum electrons were obtained from the radial Dirac equation in a modified Hartree potential. Values for all $n = 2$ angular-distribution parameters were calculated up to 2 keV. Our results for γ_{2s} and ζ_{2p} are in excellent agreement with previous nonrelativistic IPA calculations [6]. Figure 2 shows values for $\Delta\beta, \eta$, and μ ($\xi = -\eta - \mu$) obtained from our second-order IPA calculations. Primary contributions to these parameters come from $E_1 - E_3$ and $E_2 - E_2$ terms, with the octupole term contributing about 65% at 1 keV. A smaller contribution ($\approx 10\%$) comes from the $E_1 - M_2$ term.

For our measurement geometry [13], Eq. (2) and our $O(k^2)$ calculations can be used to estimate the influences

of second-order effects on the analysis of experimental results for ζ_{2p} ($= 3\delta_{2p} + \gamma_{2p}$). Specifically, an effective value of ζ , including these influences, can be defined as

$$(\zeta)_{\text{eff}} = \sqrt{\frac{27}{2}} \left[\frac{\sigma(\theta_m, 0)}{\sigma(\theta_m, \pi/2)} - 1 \right] \approx \frac{\gamma + 3\delta + \sqrt{54}(\mu - 7\xi/18)}{1 - \mu}, \quad (3)$$

using the notation $\sigma(\theta, \phi) = \frac{d\sigma}{d\Omega}(\theta, \phi)$. Using the results in Fig. 2, ζ_{eff} for $2p$ and γ_{eff} for $2s$ can be determined and compared to the results in Fig. 1 to identify influences of second-order nondipole effects. (We stress the measurements are fine, only the assumptions behind their analysis are suspect.) This exercise yields the dotted curves in Fig. 1, providing excellent agreement with γ_{2s} and clearly improved agreement with ζ_{2p} . The second-order corrections contained in ζ_{eff} account for much of the difference between the first-order theory and experiment for ζ_{2p} , demonstrating the first observation of $O(k^2)$ effects in soft-x-ray photoemission.

To confirm this unexpected finding, we made additional measurements with our apparatus, which contains four electron analyzers in a chamber which can rotate about the photon beam. At a nominal angular position, two analyzers are at θ_m and $\theta = 0^\circ$ in the plane perpendicular to the photon beam ($\phi = 90^\circ$), which we refer to as the dipole plane because first-order corrections vanish, while the other analyzers are positioned on the 35.3° cone in the forward direction with respect to the photon beam, with one of them at θ_m and $\phi = 0^\circ$. Photoemission intensities in the magic-angle analyzers are independent of β and can differ only because of nondipole effects. While the magic angle is no longer strictly valid when second-order effects are included, calculations show they can be unimportant in certain geometries (see below).

New measurements were performed at ten rotational positions, yielding 20 angle-resolved intensities for Ne $2s$ and $2p$ photoemission at different angles θ within the dipole plane, and 20 more at different angles θ and ϕ around the nondipole cone. From the calculated results for $\Delta\beta_{2p}$ in Fig. 2, direct second-order effects on β_{2p} should be insignificant; $\Delta\beta_{2p} \approx 0.005$ near 1 keV, much smaller than our measurement uncertainties. Therefore, values of β_{2p} determined from the dipole-plane spectra should agree well with DA calculations, *if* effects due to η , μ , and ξ are negligible in the dipole plane. Using Fig. 2, the influence of these parameters on angle-resolved photoemission intensities can be predicted. In the dipole plane, we predict their effects will mostly cancel, and thus the excellent agreement [10] between experiment and theory for β_{2p} is not surprising.

In the nondipole cone, influences of the second-order parameters are superimposed on intensity variations due to the dipole β and the first-order δ and γ parameters.

However, for both $2s$ and $2p$, our calculations predict effects due to η , μ , and ξ also mostly cancel around the nondipole cone. Furthermore, small residual effects around this cone are similar in sign and magnitude for $2s$ and $2p$, which is relevant because intensity ratios are the raw input for data analysis. Assuming no influence of second-order effects in the nondipole cone, we modeled the measured $2s/2p$ ratios around this cone using Eq. (1) to derive values for γ_{2s} and ζ_{2p} . These results (solid circles in Fig. 1) agree extremely well with first-order calculations [6,7,11], confirming our prediction of near cancellation of second-order effects in this geometry.

The above confirmation tests include two independent experimental methods to determine γ_{2s} and ζ_{2p} : one relies on measurements at many angles in the nondipole cone, the other relies on comparison of magic-angle-only measurements in the dipole plane and the nondipole cone. For the former, second-order effects mostly vanish. For the latter, in contrast, the influences of η , μ , and ξ on Ne $2p$ photoemission are expected to be opposite in sign for $\phi = 0^\circ$ and $\phi = 90^\circ$, because of the $\cos(2\phi)$ terms in Eq. (2). Thus, second-order effects should be observable with the latter method, hence the differences in values for ζ_{2p} derived using the two methods.

As a demonstration of the influence of second-order nondipole effects on angle-resolved-photoemission intensities, Fig. 3 compares spectra taken with the two magic-angle analyzers. Figure 3a contains a neon photoemission spectrum taken at $\hbar\omega=1200$ eV, θ_m , and $\phi = 90^\circ$ in the dipole plane, where influences of β , δ , and γ vanish. Included are fit curves showing modeled peak shapes and photoemission satellites to the left of the $2s$ peak. The overall fit (solid curve) matches the data very well, as indicated by the residual in Fig. 3b.

This spectrum and fit are reproduced in Fig. 3c and compared to a nondipole-cone spectrum at 1200 eV, θ_m , and $\phi = 0^\circ$. Intensity normalization between the spectra was achieved using γ_{2s} from Fig. 1, for which experiment and theory agree well. By inspection, the $2s/2p$ ratio is different in the two spectra. One possible explanation is a differential influence of first-order nondipole effects on the $2s$ and $2p$ intensities. As a quantitative test of this hypothesis, we derived the dotted region in Fig. 3c by multiplying the fit to the $2p$ peak in the dipole-plane spectrum by the expected differential effect on $2s$ and $2p$ peak intensities in the nondipole-cone spectrum determined from IPA-/RPA-predicted values for γ_{2s} and ζ_{2p} (see Eq. (1)). If first-order effects alone explain the observed variation of the $2s/2p$ ratio, then the dotted region should coincide with the $2p$ peak in the nondipole-cone spectrum. It does not, and thus the difference between the dotted region and the open-circle data ($\approx 10\%$) is attributed to the influence of second-order effects.

In conclusion, an experimental and theoretical study of valence photoemission from neon has demonstrated the

first observation of second-order (primarily $E_1 - E_3$ and $E_2 - E_2$) nondipole effects on photoelectron angular distributions in the soft-x-ray region. A general expression for the differential photoionization cross section, including all contributions through second order, has been derived in a form convenient for comparison to experiment.

This work was supported by NSF and DOE EPSCoR. AD and WRJ were supported in part by NSF grant PHY-99-70666. DWL acknowledges UNLV Sabbatical Leave support. The experiments were performed at the Advanced Light Source at Lawrence Berkeley National Lab., supported by the DOE Materials Science Division, BES, OER under contract DE-AC03-76SF00098.

* Present address: ITAMP, Harvard-Smithsonian Center for Astrophysics, Cambridge, MA 02138.

- [1] H. A. Bethe and E. E. Salpeter, *Quantum Mechanics of One- and Two-Electron Atoms* (Springer-Verlag, Berlin, 1957).
- [2] B. Krässig, M. Jung, D. S. Gemmell, E. P. Kanter, T. LeBrun, S. H. Southworth, and L. Young, *Phys. Rev. Lett.* **75**, 4736 (1995); M. Jung, B. Krässig, D. S. Gemmell, E. P. Kanter, T. LeBrun, S. H. Southworth, and L. Young, *Phys. Rev. A* **54**, 2127 (1996).
- [3] O. Hemmers, P. Glans, D. L. Hansen, H. Wang, S. B. Whitfield, D. W. Lindle, R. Wehlitz, J. C. Levin, I. A. Sellin, R. C. C. Perera, E. W. B. Dias, H. S. Chakraborty, P. C. Deshmukh, and S. T. Manson, *J. Phys. B* **30**, L727 (1997).
- [4] H. K. Tseng, R. H. Pratt, S. Yu, and A. Ron, *Phys. Rev. A* **17**, 1061 (1978).
- [5] D. W. Lindle and O. Hemmers, *J. Electron Spectrosc.* **100**, (1999) in press, and references therein.
- [6] J. W. Cooper, *Phys. Rev. A* **47**, 1841 (1993); **42**, 6942 (1990).
- [7] A. Bechler and R. H. Pratt, *Phys. Rev. A* **42**, 6400 (1990); **39**, 1774 (1989).
- [8] W. R. Johnson and C. D. Lin, *Phys. Rev. A* **20**, 964 (1979); W. R. Johnson and K. T. Cheng, *ibid.* **20**, 978 (1979).
- [9] M. Ya. Amusia and N. A. Cherepkov, *Case Studies in Atomic Physics* (North-Holland, Amsterdam, 1975), Vol. 5, p. 155.
- [10] E. W. B. Dias, H. S. Chakraborty, P. C. Deshmukh, S. T. Manson, O. Hemmers, P. Glans, D. L. Hansen, H. Wang, S. B. Whitfield, D. W. Lindle, R. Wehlitz, J. C. Levin, I. A. Sellin, and R. C. C. Perera, *Phys. Rev. Lett.* **78**, 4553 (1997).
- [11] W. R. Johnson, A. Derevianko, K. T. Cheng, V. K. Dolmatov, and S. T. Manson, *Phys. Rev. A* **59**, 3609 (1999).
- [12] A. Derevianko, W. R. Johnson, and K. T. Cheng, *At. Data Nucl. Data Tables* **74** (1999) in press. The parameters λ , μ , and ν in this work have been replaced here by η , μ , and ξ to avoid confusion with photon wavelength

and frequency.

- [13] O. Hemmers, S. B. Whitfield, P. Glans, H. Wang, D. W. Lindle, R. Wehlitz, and I. A. Sellin, *Rev. Sci. Instrum.* **69**, 3809 (1998).

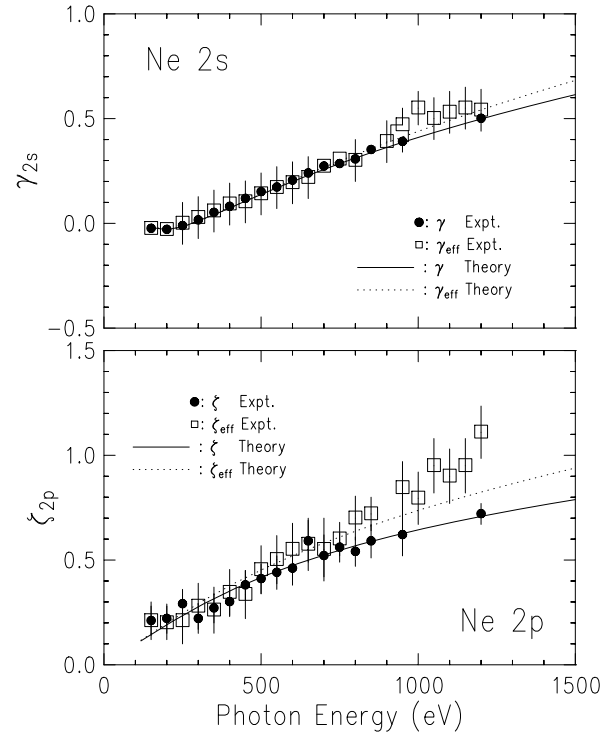


FIG. 1. Experimental and theoretical values of γ_{2s} and ζ_{2p} ($3\delta_{2p} + \gamma_{2p}$) for neon. The effective quantities include second-order [$O(k^2)$] nondipole influences. See text for complete description.

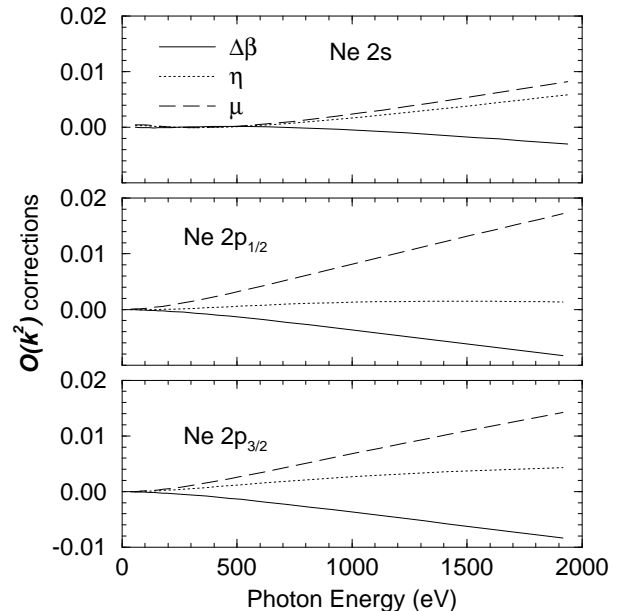


FIG. 2. Nondipole parameters of $O(k^2)$ for neon.

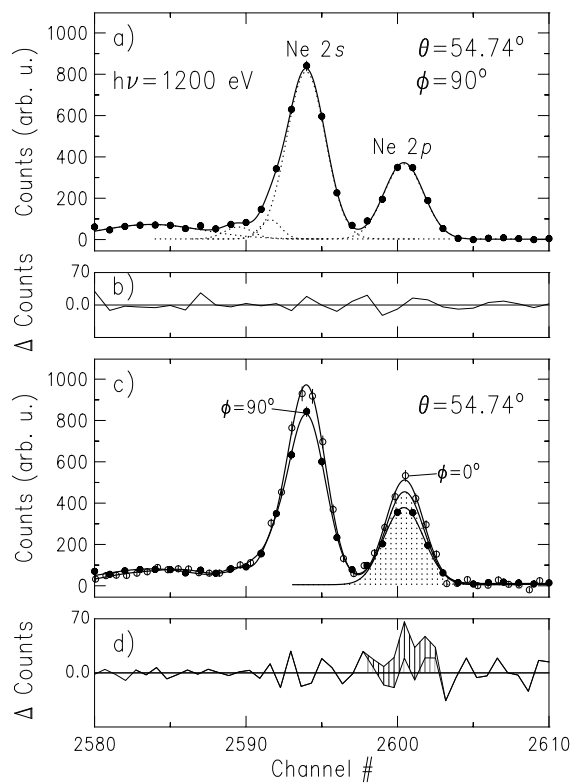


FIG. 3. Valence photoemission spectra of neon taken at 1200 eV and $\theta_m = 54.7^\circ$. a) $\phi = 90^\circ$ spectrum, including a fit. b) Residual of fit in (a). c) Same spectrum and fit as in (a) compared to a $\phi = 0^\circ$ spectrum. d) Residual of fit to the $\phi = 0^\circ$ spectrum (lower curve), and difference between the $\phi = 0^\circ$ fit and the dotted region in (c) (upper curve). The hatched area is $2p$ photoemission intensity attributable to second-order corrections. See text for full explanation.